THE JOURNAL OF PHYSICAL CHEMISTRY B

Article

pubs.acs.org/JPCB

Myoglobin Unfolding in Crowding and Confinement

Ashima Malik,† Jayanta Kundu,† Sanjib K Mukherjee, and Pramit K Chowdhury*

Department of Chemistry, Indian Institute of Technology Delhi, Hauz Khas, New Delhi 110016

Supporting Information

ABSTRACT: Crowding and confinement have often been used synonymously with regard to their effect on the structure and dynamics of proteins. In this work, we have investigated the unfolding of the protein myoglobin (Mb) entrapped in the confinement of the water pool of AOT reverse micelles and in the presence of some commonly used macromolecular crowding agents (Ficoll 70, Dextran 70, and Dextran 40). Our results reveal that confinement effects can be quite destabilizing in nature for Mb with the extent of distortion depending on a host of factors apart from the size of the confining cage. Effects of the crowding agents on myoglobin also show a deviation from the general notion that synthetic macromolecular crowding agents are always stabilizing in nature. Ficoll 70 was observed to be particularly destabilizing in its influence on Mb unfolding. Moreover, tryptophan lifetime studies point to the fact that the Trp−heme distance in Mb might not always be a reliable probe of the secondary structural dissolution of the protein.

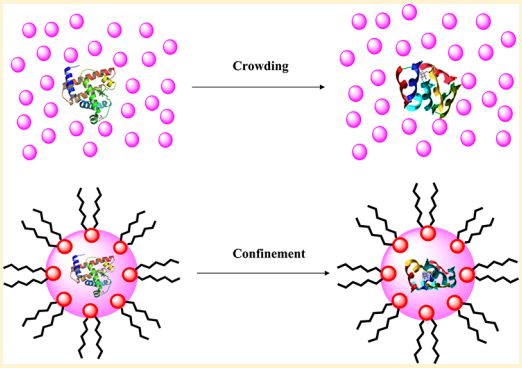

INTRODUCTION

In the living system proteins are known to perform their specific functions in a medium containing a high concentration of macromolecules (50−400 g/L) composed of DNA, RNA, lipids, and other proteins.[1,2] These macromolecules, often referred to as crowding agents, occupy a large portion of the volume of the cell, thus excluding this space to other biomolecules,[3−13] and thereby giving rise to the phenomenon commonly known as "excluded volume effect". Crowding has been shown to affect a multitude of processes like protein aggregation,[7,9] protein−protein interaction,[8] and protein diffusion[9−13] and has been steadily gaining in importance in recent years. One of the areas wherein macromolecular crowding has made appreciable impact is protein structure and stability. Denatured populations of proteins in general occupy larger conformational spaces as compared to the native structural ensemble and hence are likely to be more affected by the excluded volume phenomenon presented by the crowded medium. Thus macromolecular crowding agents entropically destabilize the unfolded state, thereby shifting the equilibrium toward the folded protein leading to increased stability. Evidence with regard to this entropy stabilization mechanism (ESM)[14] can be found in a number of studies wherein the crowding agents (often in a concentration dependent manner) bring about an increase in the thermal denaturation midpoint T_m (and/or C_m, the midpoint of chemical denaturation) of the protein or peptide under investigation.[2,15−18] However, a recent report shows that proteins when used as crowding agents can be destabilizing in nature.[19] Moreover, besides directly influencing the conformational subspace of the denatured ensemble, both simulations and experiments have also provided evidence toward native-state modulation of proteins in the presence of crowders,[2,20] even leading to a dramatic increase in catalytic efficiency for enzymes.[21]

Similar to a crowded scenario is the effect of confinement on the stability and dynamics of proteins. Confinement involves physical entrapment of the concerned biomolecule within the rigid walls of cavities of different shapes (e.g., spherical, cylindrical) and sizes.[22] Sequestration of proteins in the pores of sol−gel matrix has revealed that confinement can affect both the native structure and stability of proteins, with α-lactalbumin showing an almost 30 °C increase in its thermal melting temperature.[23] Confinement like crowding disallows those conformations that exceed the dimensions of the confining space, thereby reducing the available free space to the entrapped biomolecule. Theoretical models solely based on entropy considerations predict that in confined spaces that are of approximately the same dimensions as of the native protein, the stabilization observed is far greater than that encountered in the case of the crowding agents.[24] This disparity has been attributed to density fluctuations that can lead to interstitial voids (along with those already present based on the packing density of the respective crowding agent) in solutions of crowding agents, thereby allowing transient spaces where unfolded chains can extend into.[25] Chaperonin-induced cage-like confinement is also known to bring about enhanced stability of proteins along with acceleration of the folding process.[26] A recent simulation study has shown that the extent of stabilization of the folded ensemble relative to that of the unfolded state can be described using a scaling law involving the size of the confining space.[27] Confinement can also lead to destabilization of proteins

Received: October 26, 2011
Revised: September 29, 2012
Published: October 1, 2012

   dx.doi.org/10.1021/jp306873v | J. Phys. Chem. B 2012, 116, 12895−12904

as was revealed by another simulation study wherein protein helices were denatured when confined within a nanotube.[28]

In this work we have studied the unfolding of myoglobin (Mb) in both confined and crowded environments to investigate their effects on the denatured conformational ensemble of the protein. Myoglobin is one of the most well-studied proteins and has long been serving as a model for the folding and unfolding of heme proteins. It is a small, compact globular protein having eight α helices (A-H) and is composed of 153 amino acids cradling a heme prosthetic group with iron in center surrounded by a hydrophobic core.[29] A distinct advantage of studying the unfolding of myoglobin (Mb has two intrinsic tryptophan residues) is that tryptophan (Trp) fluorescence intensity and lifetime are direct evidence of the local conformational distribution because Trp and heme constitute an effective intrinsic energy transfer pair.[30] To investigate the effects of crowding, we have employed the commonly used synthetic polymers Ficoll 70, Dextran 40, and Dextran 70. These are neutral, highly branched polysaccharide units showing ready dissolution in water and are known to be inert in nature toward the biological macromolecules.[31] To study the confinement effect on Mb, AOT reverse micelles formed by dissolving sodium bis(2-ethylhexyl) sulfosuccinate (AOT) in isooctane have been chosen. Beyond the critical micellar concentration, the AOT molecules assemble in isooctane (IO) in a manner that the hydrophobic tails point outside into the bulk organic solvent whereas the polar sulfosuccinate head groups point inside to give rise to a polar core.[32] The presence of the latter is of great significance as water added to the system will be sequestered directly inside the polar core (hence the latter is also referred to as the water pool). One of the critical parameters characterizing the reverse micelles is the size of the water pool, which in turn is governed by the molar ratio of water to AOT (w_0 = [H_2O]/[AOT]).[33−37] Thus along with changing the size of micellar pool by varying the amount of water added to the system, the AOT/IO/H_2O reverse micelles also offers us the unique opportunity of modulating the dimensions of the confining compartment, thereby allowing a direct readout on the effect of confinement on the conformation of the encapsulated proteins. Here we have solubilized Mb in the reverse micellar water pools and have subsequently investigated the unfolding of the protein as a function of chemical and thermal denaturation. Not only is the native structure of Mb observed to be distorted extensively inside the AOT water pools as compared to that in buffer, but also the denaturation transition profiles are drastically altered. On the other hand, the crowding agents did not seem to perturb the Mb unfolding profile dramatically; however, one of the crowders employed was found to be destabilizing for the protein under all conditions. Our results also reveal that a direct comparison between confinement and crowding is difficult in the present case as the nature of the underlying interactions can be quite different.

MATERIALS AND METHODS

Myoglobin from equine skeletal muscle was purchased from Sigma-Aldrich Chemical Co. (USA) and was used as received without further purification. Urea, Ficoll 70, Dextran 70, and Dextran 40, were also purchased from Sigma-Aldrich and used as received. Sodium phosphate dibasic (Na_2HPO_4) anhydrous and monobasic (NaH_2PO_4) dihydrate were purchased from Merck Specialties Private Limited (Mumbai, India). Aerosol-OT (AOT, sodium bis(2-ethylhexyl) sulfosuccinate) of 99% purity was obtained from Sigma-Aldrich and was further purified by dissolving in methanol and stirring overnight in the presence of activated charcoal. Subsequent filtration and removal of methanol yielded solid AOT; the process was repeated three times and AOT was then dried under vacuum to make sure that the obtained AOT was pure enough and suitable for use.

Preparation of Protein Solutions. Phosphate buffer solution (50 mM) of pH = 7 was prepared by dissolving weighed amounts of mono- and dibasic sodium phosphate in Millipore water (Elix 3 UV; Millipore, Molsheim, France). All myoglobin containing stock solutions were prepared in the aforesaid buffer and diluted as required before carrying out the measurements. For the chemical denaturation experiments, a series of urea solutions were prepared in the phosphate buffer; the actual concentration of urea was then determined by measuring the corresponding refractive indices using a refractometer (KRUSS, A Kruss Optronic, GERMANY). For the experiments with different concentrations (100 and 200 g/L) of macromolecular crowders, Ficoll 70, and Dextran (70 and 40) were dissolved in phosphate buffer after weighing out the appropriate amounts using a Precisa XB 120A (Sweden) analytical balance to get the desired concentration. The reverse micelle solutions with varying w_0 values (4, 8, 12, and 16) were prepared by injecting a desirable volume of phosphate buffer (with or without protein) into a 50 mM AOT/isooctane solution. The samples were then centrifuged to remove undissolved species if any. The concentration of myoglobin was measured with the help of a UV−visible spectrophotometer (Model UV-2450, Shimadzu) in the range of 200−700 nm. The molar extinction coefficients used for myoglobin are as follows: 13 980 M^{-1} cm^{-1} at 280 nm and 188 000 M^{-1} cm^{-1} at 409 nm (the soret band).[38,39] For the chemical denaturation studies inside AOT reverse micelles, the urea concentration reported is that of the solution being injected into the AOT/IO solution for a specific water loading capacity, i.e., the w_0 value. However, the final urea concentration inside the reverse micellar solution is expected to be very low, i.e., 0.0071, 0.0214, 0.0357 M at w_0 = 8 for 1, 3, and 5 M urea, respectively.

Steady-State Fluorescence. All fluorescence experiments were performed with the Cary Eclipse (Varian) fluorescence spectrophotometer. Tryptophan excitation was carried out at 295 nm to avoid excitation of the tyrosine residues and emission spectra were obtained in the range of 305−500 nm. The samples were taken in 1 cm quartz cuvettes, which were in turn housed in a thermostated cell holder. For temperature dependent measurements, the samples were given sufficient equilibration time before acquiring the spectra at the respective temperatures.

Circular Dichroism. Far-UV CD experiments of myoglobin were carried out using an AVIV circular dichroism spectrometer (Model 420SF, Lakewood, NJ, USA). The samples were contained in quartz cuvettes of 1 mm path length. For urea (0−8 M) induced chemical denaturation of myoglobin in the presence and absence of macromolecular crowding agents, the Mb concentration was kept at 20 μM (or 25 μM wherever indicated) and the CD data were collected at 25 °C at 1 nm intervals. All reported spectra are an average of ten scans. Wherever the spectra were presented having the units of mean residual ellipticity, θ_{MRW} (deg cm^2 $dmol^{-1}$), the latter was calculated as θ_{MRW} = MRWθ_{obs})/10lc where θ_{obs} is the observed ellipticity in degrees, c is the concentration in moles per liter, and l is the optical path in centimeters. In the above equation MRW is the mean residue weight and is given by MRW = $M/(N-1)$, where M is the molar mass of the protein and N is the number of amino acids.[40] Thermal denaturation of myoglobin in the absence and presence of urea with or without macromolecular crowding agents was monitored at 222 nm at a scan rate of 2 °C/min. Temperature

was varied from 14 to 96 °C (for samples without urea), 10 to 96 °C (for 1 M urea), 10 to 90 °C (2 and 3 M urea), and 10 to 80 °C (4 and 5 M urea); the reason for the use of different temperature ranges for different samples was to minimize the effects of aggregation. To check the effect of scan rate on the transitions, the thermal denaturations were also carried out at the scan rate of 1 °C/min; however, no remarkable difference was observed in the unfolding profiles based on the difference in scan rates. Hence the thermal denaturation data reported are those collected at 2 °C/min.

Reversibility of the thermal transitions (in the presence and absence of urea) was also checked. First a far-UV CD spectrum of the sample was scanned (190−260 nm) at the starting temperature and then the thermal denaturation was carried out up to that temperature, which marks the beginning of unfolded baseline. The sample was then allowed to cool to the starting temperature, after which a far-UV CD spectrum was again recorded. The ellipticity and shape of the spectra before and after heating were then compared. In buffer only (i.e., in the absence of crowding agents) and in the presence of Ficoll 70, the thermal denaturation curves showed more than 95% and 80% reversibility, respectively, whereas for Dextran 40 and 70 the transitions were found to be irreversible. Thus the thermal unfolding curves of buffer and Ficoll 70 were fitted according to the following equations to obtain the thermal midpoint (T_m), enthalpy (ΔH_m), and entropy (ΔS_m) of unfolding, and the change in heat capacity (ΔC_p) for the aforementioned samples:

$$y = \frac{y_F(T) + K_{eq} y_U(T)}{1 + K_{eq}} \quad (1)$$

$$K_{eq} = \exp[-\Delta G(T)/RT] \quad (2)$$

$$\Delta G(T) = \Delta H_m + \Delta C_p(T - T_m) - T[\Delta S_m + \Delta C_p \ln(T/T_m)] \quad (3)$$

$$y_F(T) = a_F + b_F T \quad (4)$$

$$y_U(T) = a_U + b_U T \quad (5)$$

where y is the spectroscopic signal (CD), y_F and y_U are those due to the folded and unfolded baselines, b_F and b_U are the slopes, and a_F and a_U are the intercepts of the pretransition and post-transition baselines, respectively. T_m is the thermal denaturation midpoint and K_{eq} is the equilibrium constant for the unfolding of the protein. The folded and unfolded baselines have been assumed to vary linearly with temperature. All the thermodynamic parameters have been provided in Table 3.

Time resolved Fluorescence. Excited-state lifetime measurements were performed using a time-correlated single photon counting (TCSPC) spectrometer (Edinburgh FLS920). For our experiments a LED having its central wavelength at 284 nm was used as the source for exciting the Tryptophan (Trp) residues of Mb. Emission was subsequently collected at 330 nm (for the reverse micelle samples) and at 360 nm (for Mb in buffer with and without the crowding agents) through a single monochromator with a 10 nm bandpass over a total time range (TAC) of 20 ns for all samples. Emission decays were fit with appropriate instrument response functions (IRF) collected using a scattering solution. The FWHM (full width at half-maximum) of the IRFs collected was typically in the range of ∼500 ps. The average tryptophan lifetime was calculated using the formula $\langle\tau\rangle = \sum_i \alpha_i \tau_i$ (α_i = amplitude and τ_i = decay time of component i).

DLS Measurements. Dynamic light scattering experiments were performed to determine the hydrodynamic diameters of AOT microemulsions (in the presence and absence of Mb) at 25 °C in a temperature controlled cell holder. The measurements were performed using a particle−size analyzer (Model Nano ZS90, Malvern Instruments, UK). The protein concentration was kept at 8 μM during the measurements.

RESULTS AND DISCUSSION

Myoglobin (Mb) Unfolding in Confinement. Thermal denaturation of Mb in AOT/IO/H_2O(buffer) reverse micelles (used as a medium to confine the protein) was carried out as a function of w_0, the latter being varied from 4 to 12. Figure 1A shows the intrinsic Trp fluorescence spectra of Mb with an increase in temperature at w_0 = 4, wherein the Trp intensity shows a decreasing trend until 90 °C, the last temperature at which the unfolding was monitored. This trend is in stark contrast to that normally observed in buffer wherein the Trp intensity shows a sudden increase (after an initial decreasing trend) due to Trp−heme separation resulting from the cooperative unfolding of Mb (Figure 1B). It is well-known that tryptophan and heme form an effective Förster resonance energy transfer (FRET) pair and thus in native Mb, the Trp intensity is severely quenched due to the proximity of the donor and acceptor moieties.[30] Myoglobin has two tryptophan residues, at positions 7 (W7) and 14 (W14) that are highly conserved across different species. Both these Trp residues are present on the A-helix of Mb near the N-terminus of the protein, with the distances from the heme cofactor being ∼21 and ∼15 Å for W7 and W14, respectively.[30] Because these Trp residues contribute to the overall fluorescence of Mb, the emission spectra or fluorescence profiles we refer to in this study are a combined response from W7 and W14. Upon unfolding the protein, the distance between the aforesaid intrinsic FRET pair(s) increases, thereby bringing about a decrease in the energy transfer

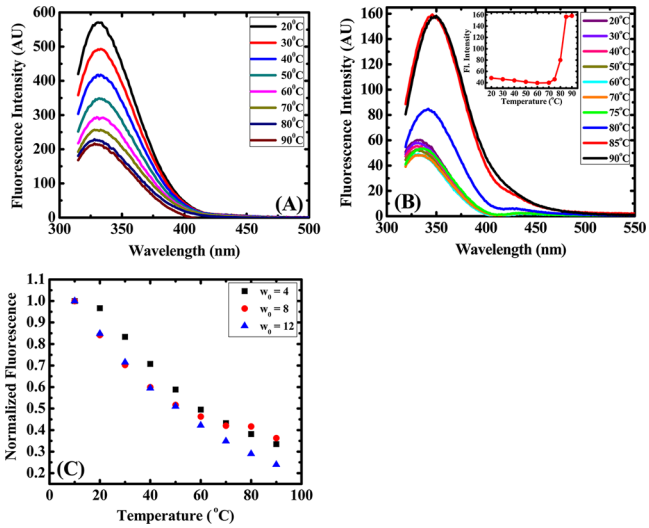

Figure 1. Temperature dependent fluorescence spectra of myoglobin (7 μM) in (A) w_0 = 4 and (B) buffer (the thermal unfolding profile monitored at λ_{em} = 350 nm shown in the inset). (C) Normalized thermal transition profile for Mb as a function of w_0 monitored at λ_{em} = 331 nm. The temperature was varied from 10 to 90 °C for all the samples.

dx.doi.org/10.1021/jp306873v | J. Phys. Chem. B 2012, 116, 12895−12904

efficiency and hence a subsequent increase in Trp fluorescence in buffer. The fluorescence thermal denaturation profile of the protein in water pools of w_0 = 8 and w_0 = 12 also shows a similar decreasing trend in Trp emission like that in w_0 = 4 (Figure 1C). It should be noted that an increase of w_0 value leads to an increase in the size of the water pools, with the radius of the pool for w_0 = 8 being approximately twice that of w_0 = 4 whereas the same for w_0 = 12 is about 3 times greater. Thus at higher w_0 values, the confinement effect on the protein as a result of encapsulation in the polar core of the AOT/IO/H_2O(buffer) reverse micelles should decrease. This alleviation in forced confinement should therefore result in more space being available for Mb, especially with regards to its unfolded population, leading to increased Trp−heme separation from thermal denaturation. However, our data (Figure 1C) show that for w_0 =12, the largest water pool used for monitoring the temperature induced conformational changes, the observed Trp intensity is the lowest (Supporting Information Figure 1A). Moreover, in none of the water pools do we observe an increase in Trp intensity (as a function of temperature), the latter often considered to be a characteristic feature signifying Mb unfolding (Figure 1B inset).

To further monitor the changes in secondary structure of Mb, we have also performed CD measurements on the protein confined in the water pools of the reverse micelles. The CD spectra of myoglobin in buffer resemble that of a typical α-helix with negative bands at 208 and 222 nm (Figure 2A). On encapsulation

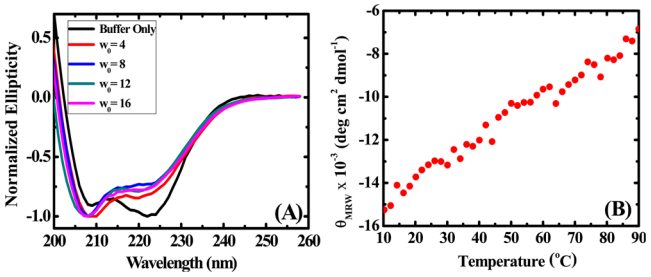

Figure 2. (A) Normalized CD spectra of Mb (7 μM) in AOT/IO/H_2O (buffer) reverse micelles at different w_0 values; the CD curves for the reverse micelle samples were normalized at 208 nm for clarity. (B) Thermal denaturation profile of myoglobin monitored at 222 nm in AOT/IO/H_2O(buffer) reverse micelle at w_0 = 8. The observed noncooperativity in the denaturation profile is conserved over a range of w_0 (=4 and 12) values.

of the protein in the water pools of varying sizes, Mb undergoes a distortion in its secondary structure as observed from the decrease in the intensity of its helical band at 222 nm (Figure 2A), in agreement with a recent study.[41] Moreover, an increase of the w_0 value and hence the size of the water pool leads to greater destabilization of the protein secondary structure. A number of factors may contribute to the aforesaid changes at the secondary structure level: (i) the water localized in the interior of the microemulsion that is known to have properties much different from those of bulk water can influence the protein conformation and/or (ii) the interaction of Mb with the interfacial wall of the AOT reverse micelle can also affect the secondary structure of the protein. Similar denaturation of another helical heme protein cytochrome *c* in AOT reverse micelles with an increase in water content of the polar core has also been observed.[42] The stability of the encapsulated Mb was further studied by monitoring the change in ellipticity at 222 nm as a function of an increase in temperature. As opposed to the cooperative transition observed for Mb in a buffer (Figure 5), the thermal denaturation profile in the AOT/IO/H_2O(buffer) reverse micelles irrespective of the w_0 values seems to be highly noncooperative (Figure 2B). A part of the reason for such a drastic change in the denaturation profile might be the underlying change in the global structure of Mb when inside the water pool of the reverse micelles as discussed above. Recent studies by Pande and co-workers have shown that confinement can lead to destabilization of helices primarily because of reduced solvent entropy within the confining space, with the assumption that the potential of the confining walls is repulsive in nature.[43] Indeed, the H-bond network within reverse micelles formed by AOT has been shown to be much different from that of bulk water and hence the water inside the water pool is quite likely to affect the protein thermodynamics.[44−46] A similar notion of confined water influencing protein structure has also been proposed by Eggers et al.[23] That the interaction of the protein with the polar wall of the water pool of the reverse micelles can also play a significant role in the destabilization of its structure has been shown in recent simulation studies wherein charged residues of proteins or peptides were found to interact with the AOT head groups.[47−49,42]

Chemical denaturation of Mb as a function of urea was also carried out in varying sizes of the reverse micellar water pool. An increase in the concentration of urea leads to, as expected, a gradual unfolding of Mb, as observed from the decrease in signal at 222 nm (Figure 3), with the sample containing 5 M urea

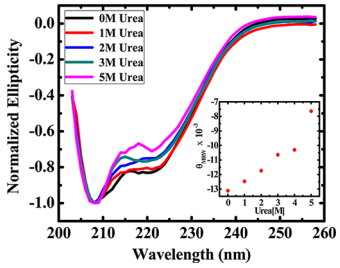

Figure 3. Normalized CD spectra of Mb (14 μM) in AOT/IO/H_2O(buffer) reverse micelles at w_0 = 8 containing different concentrations of urea (for the actual urea concentration refer to materials and methods). Normalization was carried out at 208 nm for clarity. Shown in the inset is the transition profile for Mb as a function of urea monitored at 222 nm (*Y*-axis has been represented in deg cm^2 dmol^{-1} units).

having the least helicity at that wavelength. In this regard it is surprising to note that though the actual concentration of urea in the solution is quite low (see Materials and Methods for the actual urea concentrations), it is still capable of bringing about appreciable distortion in the secondary structure of the protein. This observation points toward an enhancement in urea activity inside the reverse micellar water pool as has recently been suggested.[50] The urea induced unfolding transition (Figure 3 inset) also shows a noncooperative change similar to that obtained during thermal denaturation, thereby signifying that in both cases similar factors are instrumental in bringing about the observed noncooperativity. Unfolding of Mb inside the water pool was further confirmed through steady-state fluorescence measurements wherein the Trp emission intensity increased with urea concentration, thus showing that the Trp−heme pair(s) underwent increased separation (Supporting Information, Figure 1B).

To further probe the conformational disposition of Mb inside the reverse micelle, we performed time-resolved fluorescence studies of Trp emission as a function of different external conditions.

dx.doi.org/10.1021/jp306873v | *J. Phys. Chem. B* 2012, 116, 12895−12904

Fluorescence lifetime is a very sensitive parameter for analyzing the excited-state interactions and the local environment present around the fluorophore. The fluorescence decay(s) of Mb in AOT/IO/H_2O(buffer) reverse micelles could be well described by a biexponential fit throughout, irrespective of the different water pool sizes used. Tryptophan itself shows complicated excited-state photophysics even in buffer[51] and hence here we have used the average fluorescence lifetime ($\langle\tau\rangle$) to monitor the proximity of the Trp residues of Mb to the heme prosthetic group, in the reverse micelles. Table 1 shows the Trp lifetime as a function of the w_0 values of the AOT/IO/H_2O(buffer) system; for comparison we have also measured the lifetime of the intrinsic Trp residues of Mb in buffer as shown in Table 4. The lifetimes in the AOT reverse micelles (Table 1 and Figure 4A) are much longer than that observed in buffer (Table 4 and Figure 4B). The Trp lifetime in buffer of ~180 ps is understandably short because of the close proximity of the Trp residues to heme, resulting in a significant amount of energy transfer from Trp to the cofactor. However, the same in $w_0 = 4$ is 1.63 ns and the lifetime undergoes a gradual decrease as the w_0 value increases. This trend is quite contrary to what was expected on the basis of the fact that relaxation (increase) in the confining dimensions should bring about an expansion of the native state resulting in a decrease in energy transfer (and hence increased lifetime). These lifetime data therefore clearly show that the conformation inside the water pool of the AOT RM is quite different from that in bulk water, thus agreeing with our CD studies. One of the reasons for such a dramatic increase in the fluorescence lifetime of the intrinsic Trp residues of Mb in the reverse micelles can be the dissociation of the heme from the protein once the protein is incorporated in the water pools. Soret band absorbance studies (data not shown), however, indicate that the heme remains intact, as has also been shown in a recent study.[41] Moreover, the decrease in helicity as observed from CD (Figure 2A) in general should lead to an increase in distance between the Trp residues and the heme moiety; therefore the decrease in the Trp lifetime observed in this study with an increase in the w_0 value suggests that the distorted conformation is such that it has forced the FRET pair to come closer instead of moving further apart. The lifetime data are also in agreement with the steady-state fluorescence spectra as a function of w_0 wherein the intensity decreased as the size of water pool was increased (Supporting Information Figure 1A), implying enhanced FRET due to an increase in Trp−heme proximity. The decrease in lifetime with an increase in w_0 signifies that the protein probably does not undergo any expansion at least with respect to the Trp−heme separation. However, for cytochrome c in reverse micelles an increase in the water content inside the AOT water pool resulted in increased Trp−heme separation and hence an increase in Trp intensity.[42] Thus the fluorescence data show that nature of interactions of Mb in the AOT reverse micelle water pool is quite different from that of another heme protein cytochrome *c* entrapped in similar confinement.

Lifetime measurements were also carried out for different concentrations of urea in buffer (Figure 4B) and inside the water pool of the reverse micelles (Tables 2 and 4) to study the effect of chemical denaturation on the Trp−heme separation. In buffer as one increases the concentration of urea from 0 to 5 M, the lifetime undergoes a drastic increase; that is, it increases from 180 ps to 1.48 ns. However, the change in lifetime for Mb inside the micellar pool in the presence of urea is comparatively nominal. The change for $w_0 = 8$ is from 1.32 to 1.50 ns (Table 2A and Supporting Information Figure 2) (for 0−5 M urea) whereas that for $w_0 = 12$ is from 1.22 to 1.43 ns (Table 2B). Before ending the discussion on the lifetime measurements in AOT reverse micelles, we would like to comment on the two lifetime components reported in Tables 1 and 2 for tryptophan fluorescence. In general, the biexponential decay can be attributed to the presence of tryptophan rotamers, as has been shown in recent studies involving the proteins bovine serum albumin (BSA) and human serum albumin (HSA).[52,53] In the case of Mb, analysis of the tryptophan decay is more complicated due to the presence of FRET between the two Trp residues and the heme cofactor. Moreover, the changes we observed in the corresponding lifetime values and the associated amplitudes are also small, probably suggesting that large scale population redistribution of the Trp rotamers is not occurring in this case. This further reinforces the fact that modulation in distance between the Trp residues and the heme moiety because of small amplitude local conformational

Table 1. Fluorescence Lifetime of Myoglobin in AOT/H_2O/IO Reverse Micelle as a Function of w_0[a]

environment	a_1	τ_1 (ns)	a_2	τ_2 (ns)	av lifetime (ns)	χ^2
$w_0 = 4$	0.53	0.71	0.47	2.68	1.63	1.17
$w_0 = 8$	0.60	0.66	0.40	2.33	1.33	1.19
$w_0 = 12$	0.61	0.60	0.39	2.19	1.22	1.27
$w_0 = 16$	0.62	0.63	0.38	2.12	1.20	1.32

[a]The samples were excited at 284 nm, and emission was collected at 330 nm.

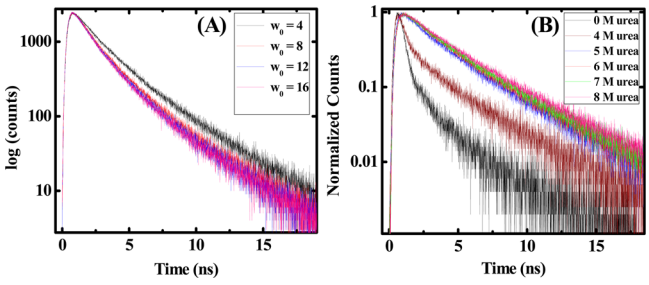

Figure 4. Fluorescence decay profiles of Mb in (A) AOT/IO/H_2O(buffer) reverse micelles as a function of different w_0 values and (B) buffer, with an increase in concentration of urea. λ_{exc}= 284 nm and λ_{em} = 330 nm (for reverse micelle) and 360 nm (for buffer).

Table 2. Fluorescence Lifetime of Myoglobin in AOT/H_2O/IO Reverse Micelle as a Function of Urea[a]

[urea] (M)	a_1	τ_1 (ns)	a_2	τ_2 (ns)	av lifetime (ns)	χ^2
(A) w_0= 8						
0	0.60	0.66	0.40	2.33	1.32	1.19
1	0.59	0.68	0.41	2.44	1.40	1.23
3	0.59	0.74	0.41	2.64	1.52	1.16
5	0.61	0.67	0.39	2.80	1.50	1.33
(B) w_0= 12						
0	0.61	0.61	0.38	2.20	1.23	1.27
1	0.61	0.60	0.39	2.29	1.26	1.27
3	0.60	0.61	0.40	2.48	1.36	1.20
5	0.61	0.56	0.39	2.78	1.43	1.19

[a]The samples were excited at 284 nm, and emission was collected at 330 nm.

dx.doi.org/10.1021/jp306873v | J. Phys. Chem. B 2012, 116, 12895−12904

changes in Mb is the main reason behind the observed trend in fluorescence lifetimes.

DLS studies were performed to investigate the changes in the micellar size on protein incorporation in the absence and presence of urea. Our data show that protein entrapment in the reverse micelle water pool does not give rise to a dramatic change in the hydrodynamic radius of the micelle (Supporting Information Table 1). With the hydrodynamic diameter (D_h) of Mb being approximated as ~2.42 nm[54] and this being comparable to that of the micelle, it seems therefore that at the lower w_0 values, Mb does face severe confinement inside the water pools.

Myoglobin Unfolding in the Presence of Macromolecular Crowders. CD measurements for both thermal and chemical denaturation reveal varying effects of the crowders on the unfolded ensemble of Mb. Thermal denaturation reveals that all the crowders at the concentration of 200 g/L have a destabilizing effect on Mb as compared to that in buffer (Figure 5A).

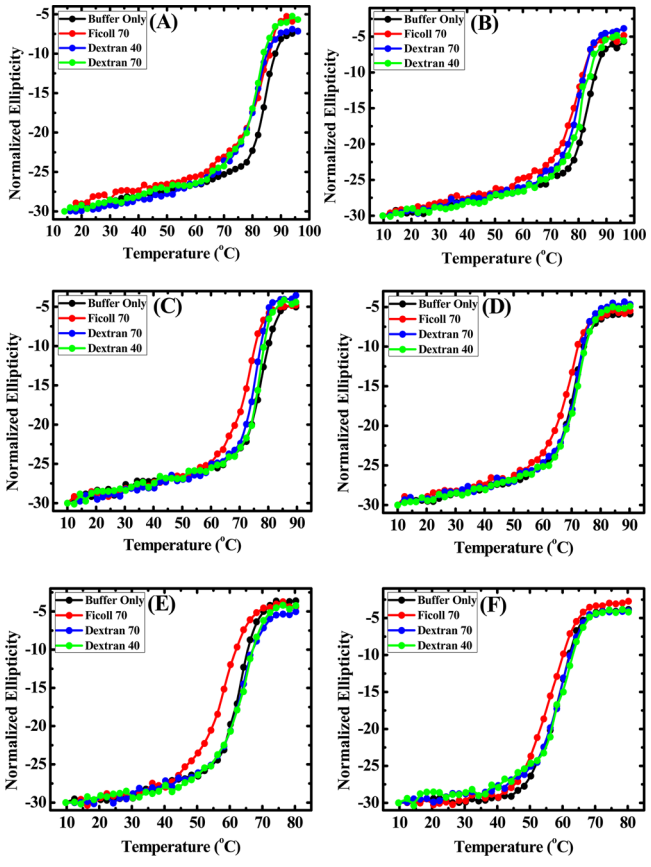

Figure 5. Thermal denaturation of Mb in the presence of (A) 0 M urea, (B) 1 M urea, (C) 2 M urea, (D) 3 M urea, (E) 4 M rrea, and (F) 5 M urea monitored at 222 nm using CD in the presence of various crowding agents (200 g/L) as noted in the figure panels. The solid lines should just be regarded as aides to follow the transition. The concentration of Mb was 20 μM for (A) whereas, for the ones having urea, the protein concentration was kept at 25 μM.

These findings are quite different from what has been observed in general for proteins in the presence of macromolecular crowding agents with proteins like ubiquitin,[16] cytochrome *c*,[15] and apoflavodoxin,[2] all showing an increase in denaturation midpoint values. Thermal denaturation studies at the lower concentration (100 g/L) of crowding agents also gave very similar transition profiles, implying that the crowding agent concentration has a negligible effect on the nature of the observed transition (Supporting Information Figure 3).

Mb is quite stable at room temperature, as observed from the high thermal denaturation midpoint value (T_m) of ~85 °C in buffer (Table 3), thereby giving rise to an incomplete unfolded baseline in the thermal denaturation experiments. Because it is assumed that the macromolecular crowding agents exert their influence mainly through the excluded volume effect, it is possible that the observed trend in Figure 5A might be arising from incomplete denaturation of the protein. Indeed, a recent study has shown that crowding effects on the thermal stability of cytochrome *c* were enhanced when the protein was initially destabilized with a chemical denaturant.[17] Hence to increase the extent of thermal denaturation within the accessible temperature range, thermal unfolding experiments of Mb in the presence of 1−5 M urea were also carried out (Figure 5B−F). At the aforesaid concentrations of 1−4 M, urea has negligible effects on the native secondary structure of Mb whereas at 5 M the protein's secondary structure dissolution appears to have just been initiated (Supporting Information Figure 4). As expected, thermal unfolding data with urea reveal that the protein gets progressively destabilized with increasing urea concentration with the T_m shifting to lower values (Table 3 and Supporting Information Figure 5). Additionally, this urea induced destabilization also ensures the presence of an appreciable amount of denatured protein molecules, thereby increasing the chances of the crowding agents exerting their excluded volume effects. Ficoll 70 shows a destabilizing effect on the Mb unfolding transition under all conditions (Figure 5 and Supporting Information Figure 3). Dextran 40 and Dextran 70 showed a slight variation with urea concentration whereby the transitions were destabilizing at 0−2 M urea and were superimposable with that of the buffer thermal denaturation transition for 3−5 M urea. Because crowding agents are known to enhance aggregation of proteins, we also checked the reversibility of the transitions and the scan rate dependence of the denaturation profiles. The thermal profiles for buffer and Ficoll 70 were observed to be >80% reversible and almost no dependence on scan rate was observed for the unfolding transitions under any of the experimental conditions. Moreover, the similarities in profiles of the thermal transitions in the presence of varying urea concentrations also suggest that aggregation is not a determining factor for the observed unfolding profiles. Thermodynamic parameters obtained from fitting the unfolding transitions have been summarized in Table 3. The enthalpy changes at the melting temperature (ΔH_m) for buffer and Ficoll are quite different, with the unfolding transitions in the presence of the crowding agent exhibiting lower ΔH_m under all conditions. Moreover the ΔC_p values also follow the same trend. The implications of the aforesaid observations are quite significant with regard to the nature of protein denaturation in the presence and absence of macromolecular crowders. Both ΔH_m and ΔC_p can be approximated to scale according to the manner in which the accessible surface area (ASA) of Mb changes while unfolding.[55] Thus a lower value of these thermodynamic parameters as obtained for Ficoll 70 suggests that the extent of change in ASA (i.e., ΔASA) is larger for buffer as compared to that in the crowding agent. Indeed, such a trend is not surprising given the fact that crowding agents are known to resist unfolding as the denatured conformations occupy more space than the native ensemble. In other words, though Ficoll 70 has been observed to be destabilizing, the aforesaid thermodynamic analyses, however, reveal that the crowding agent does exert its excluded volume effect whereby the extent of ΔASA is reduced as compared to that in buffer.

dx.doi.org/10.1021/jp306873v | J. Phys. Chem. B 2012, 116, 12895−12904

Table 3. Values of T_m and ΔH_m of Myoglobin in Buffer and Ficoll 70 in the Presence of Varying Concentrations of Urea

	T_m (°C)		ΔH_m (kcal/mol)		ΔC_p (cal/K/mol)		ΔS_m (cal/K/mol)	
[urea] (M)	buffer	Ficoll 70 (200 g/L)	buffer	Ficoll 70 (200 g/L)	buffer	Ficoll 70 (200 g/L)	buffer	Ficoll 70 (200 g/L)
0	85.2	83.4	109.5	69.9	1225.5	676.1	306.2	195.9
1	83.4	81.3	98.1	64.5	1064.7	664.3	275.6	183.0
2	75.0	72.4	90.9	62.2	1033.4	660.9	259.2	180.1
3	70.7	68.2	80.6	61.2	779.7	654.1	220.1	179.2
4	62.2	58.5	68.2	59.0	677.4	619.7	202.9	177.5
5	58.2	56.2	62.0	57.0	661.2	599.6	187.4	173.6

Table 4. Average Fluorescence Lifetime of Myoglobin as a Function of Urea in the Presence of Various Crowding Agents[a]

	av lifetime (ns)						
		Ficoll 70		Dextran 70		Dextran 40	
[urea][b] (M)	buffer only	100 g/L	200 g/L	100 g/L	200 g/L	100 g/L	200 g/L
0	0.18	0.20	0.25	0.27	0.26	0.19	0.27
4	0.48	0.48	0.45	0.44	0.29	0.38	0.37
5	1.48	2.50	2.22	0.55	0.57	0.83	0.88
6	2.75	2.98	2.78	1.41	1.77	3.06	2.96
7	2.92	3.14	3.04	3.04	3.05	3.32	3.39
8	3.14	3.29	3.20	3.20	3.31	3.50	3.68

[a]The samples were excited at 284 nm, and emission was collected at 360 nm. [b]From 0 to 4 M urea, the change in lifetime of Trp was very small under all conditions, signifying negligible changes in the Trp−heme distance. Hence the lifetimes for the urea concentrations between 0 and 4 M have not been included in the table.

Indeed, the maximum percentage change in ΔH_m for Mb in buffer between 0 and 5 M urea is ∼43% whereas the same for the protein in Ficoll decreases only by ∼18%.

Because CD studies report on the global conformational changes of proteins, to have a deeper insight into conformational changes taking place locally, we monitored the fluorescence lifetime of the Trp residues of Mb as a function of urea concentration. Table 4 provides comparative data of the Trp intensity decays in the absence and presence of different crowding agents as a function of urea. As expected, an increase in urea concentration is accompanied by an increase in the Trp lifetime because of the FRET donor−acceptor pair(s) (Trp−heme) moving farther away from each other. Although for 0 and 4 M denaturant concentrations the Trp lifetimes are comparable for all (consistent with the CD data wherein there is negligible change in secondary structure in this range), differences become quite pronounced at higher concentrations of urea. To better represent the overall picture, we have plotted the average lifetime values of Trp as a function of urea in the presence of the macromolecular crowders used (Figure 6A,B). Consistent with the CD

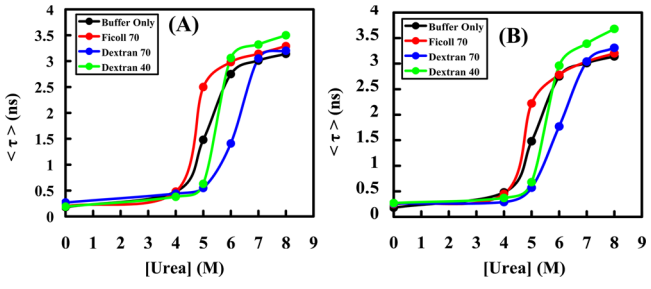

Figure 6. Average lifetime ($\langle\tau\rangle$) plot of Mb as a function of urea in the presence of (A) 100 g/L and (B) 200 g/L of various crowding agents.

denaturation data, the lifetime plot exhibits cooperative unfolding transition(s) for Mb under all solvent conditions, signifying that the Trp lifetime and hence the change in Trp−heme distances (in this study we are seeing a combined effect of change in distances of both the tryptophan residues in Mb) qualitatively matches the overall denaturation profile of the protein's secondary structure. Before 4 M and beyond 6 M urea, the average lifetime shows a gradual change, thereby representing the folded and the unfolded baselines, respectively (similar to CD). In the presence of Ficoll 70 at 100 and 200 g/L, the Trp−heme separation increases earlier, as compared to buffer and the Dextran based crowding agents, further confirming the destabilizing effect of the Ficoll observed in the CD unfolding transitions (Figure 5). Dextran 70 exhibits significant amount of stabilization to denaturation with respect to the Trp−heme separation. The average lifetimes for buffer (no crowding agent), Ficoll 70, and Dextran 70 almost overlap with each other in the unfolded ensemble corresponding to 7 and 8 M urea; however, Dextran 40 consistently shows a higher lifetime in the same region signifying greater Trp−heme separation than the others. Taken together these results reveal that Dextran 70 provides the maximum resistance to the Trp−heme separation whereas Ficoll the least. Dextran 40 based on previous studies[56] was expected to provide the maximum compaction, it being a smaller crowding agent. However, the Trp−heme separation though the largest for Dextran 40, does not necessarily portray a more extended conformation of the protein. It might be that the better packing efficiency (among the crowders used in this study) of Dextran 40 forces the Mb molecules to assume a different set of conformations in the unfolded state wherein the Trp and heme are at a greater distance as compared to the other solvent conditions studied here (similar to that observed in confinement inside the AOT water pools discussed before, wherein increased structural distortion of the protein was accompanied by a decrease in Trp lifetime).

The aforesaid lifetime analyses therefore provide some very interesting insights into the denaturation process of Mb in the presence of the crowding agents. The Trp lifetime being dependent on the Trp−heme distance is a signature of the local fluctuation(s) (as noted earlier) of the protein as opposed to the

dx.doi.org/10.1021/jp306873v | J. Phys. Chem. B 2012, 116, 12895−12904

global conformation changes reported by the CD transitions. Comparison with the urea induced CD transitions shows that the $\langle\tau\rangle$ profile for Dextran 70 is different in that it shows distinct stabilization proving that the Trp lifetime as dictated by the Trp−heme distance, does not necessarily have to follow the dissolution of the secondary structure. Also, the differential behavior of Ficoll and Dextran(s) is quite striking. Ficoll 70 seems to have a destabilizing influence irrespective of the nature of probe used; in other words the Trp lifetime and hence the Trp−heme distance are in accordance with the profiles obtained via chemical and thermal denaturation of Mb. This is quite unlike that observed for Dextran 70 wherein the Trp−heme distance lagged behind the change in secondary structure of the protein. Indeed previous studies have acknowledged the fact that the rod-shaped Dextran molecules exclude more volume to the protein molecules than Ficoll, the latter often being modeled as a semirigid sphere.[2]

SUMMARY AND CONCLUSIONS

Provided the interaction between the confining walls or macromolecular crowders and the protein is repulsive in nature, crowding and confinement have been shown to give qualitatively similar results.[25] Recent simulation studies of protein conformation and dynamics in the confinement of AOT reverse micelles by the groups of Straub and Garcia, however, show strong evidence of interaction of proteins with the surfactant molecules.[33,46,47] Confinement, as observed in this study, can lead to appreciable distortion in structure of the entrapped protein either because the size of the protein is more than or comparable to the confining cage or because of possible destabilizing interactions of the confining walls. Pande and his group have proposed an alternate theory wherein the solvent (of the confined cage) entropy can play a dominant role in determining the final structure of the protein ensemble whereby helicity of the encapsulated protein was shown to decrease.[39] In our study, the exact cause behind the structural distortion of Mb is hard to identify. Had this distortion resulted because of confinement only (assuming walls to be noninteracting), one would have seen marked changes in the secondary structure of the protein at higher w_0 values, that is, where effect of confinement should have been reduced. The fact that the increase in water content and simultaneous relaxation in the confining dimensions of the pool leads to greater reduction in the helicity of the protein implies that other factors are responsible for the observed conformational changes. Moreover, to what extent the negatively charged AOT head groups influence the final conformation can only be further rationalized by encapsulating Mb in reverse micelles that are either neutral or positively charged.

In general, short helical peptides on entrapment in AOT reverse micelles undergo a noticeable increase in helicity, this change being attributed to the lesser number of water molecules (as compared to bulk) present in the water pool to interact with the peptide backbone.[57] Thus one of the major reasons for the observed structural distortions of Mb inside the water pool might be its bigger size. Moreover, for the short alanine rich peptides, the lysine residues introduced into the peptide sequence for increasing solubility have been shown to interact with the negatively charged sulfosuccinate headgroups of the AOT molecules.[46,48] In comparison, the number of charged residues in myoglobin is much more, giving rise to increased chances of peptide−surfactant interaction thus further influencing the conformation of the protein inside the water pool. On the other hand, in the presence of the neutral macromolecular crowders, no such evidence of structural perturbation is observed for myoglobin. Moreover, the unfolding of Mb in the presence of the Dextrans and Ficoll remains predominantly cooperative whereas the same inside the water pools of the reverse micelles shows a high degree of noncooperativity as observed from the broad denaturation transitions. Although the reason for this observed noncooperative transition is not clear to us at present, we propose that it is a combination of the confined solvent (here water) having characteristics far different from bulk, and interaction of the protein with the micellar walls. Indeed such multistate noncooperative denaturation has also been observed for ubiquitin in AOT reverse micelles.[58,59]

Unfolding of Mb in the presence of crowders has also provided us with some new insights. Contrary to general observations, none of the crowding agents employed here gave rise to significant stabilization for the native state of the protein even under conditions wherein influence of excluded volume should have been apparent, i.e., when an appreciable amount of unfolded protein is present. Ficoll 70, on the other hand, was found to be destabilizing in nature, indicating that the effect of macromolecular crowders can be quite protein specific. Also, the local conformational readout of Trp−heme proximity based on the Trp lifetime reveals that short-range conformational changes need not follow the change in the global structure of the protein. For example, in the presence of Dextran 70 the Trp−heme distance change was not only found to be the most sluggish but also was quite delayed with respect to that in buffer only, as opposed to the minor stabilization observed for the same crowding agent when denatured by urea (Supporting Information Figure 5). Additionally in the presence of high urea concentration, the Trp lifetime and hence the Trp−heme distance was almost the same for buffer, Ficoll, and Dextran 70, thus further confirming the fact that the crowding agents did not provide much compaction for the denatured Mb ensemble. Such an observation might signify that the denatured state of Mb is quite compact in nature and hence does not experience the excluded volume of the crowding agents. Transient grating studies, however, have shown that the hydrodynamic radius of unfolded Mb is about 4 times greater than that of the folded Mb.[60] Furthermore, a recent study on cytochrome *c*, a 104-residue heme protein (as opposed to 153 for Mb) has shown significant stabilizing effects by the same crowding agents used by us in this investigation. Moreover, the efficiency with which the crowding agents influence the protein conformation depends on their respective shapes and sizes.[61] Although at a given crowder concentration, smaller crowding agents are known to have a greater effect than the larger ones, Dextran 70 (rod-like in shape) has been postulated to exert more effect than Ficoll 70 (spherical) based on their differences in shapes. However, it is difficult to understand why Ficoll 70 brings about a reduction in T_m for Mb in this study. Equally surprising is our observation that the enthalpy changes during the unfolding transition are much higher in buffer as compared to that of Ficoll 70. These thus suggest that though the crowding agent (Ficoll) is able to exert its excluded volume effect by decreasing the exposure of the amino acids of Mb, the protein responds in a manner such that the secondary structural dissolution takes place earlier than that compared to buffer. Dextran 40 being the smallest of the macromolecular crowders used, was also expected to bring about greater compaction and hence stabilization of the protein. However, neither the equilibrium studies nor the lifetime values match this expectation of ours. Taken together our results reveal that excluded volume effect might not be the only dominant factor determining the conformational outcome of proteins in the presence of the crowding agents. As has been suggested by a couple of recent

studies, both nonspecific interactions by crowding agents or the changing hydration pattern under high volume fractions of these crowding molecules[62] can have significant influence on the protein conformational disposition.

■ ASSOCIATED CONTENT

Supporting Information

Data obtained from the DLS measurements and a table that has details about the sizes and aggregation number of the AOT reverse micelles at different w_0 values along with the number of protein molecules per micelle. Table of changes in the free energy values for unfolding in buffer and Ficoll 70 as a function of different urea concentrations. Additional steady-state fluorescence and lifetime data for Mb in reverse micelles and CD plots for urea denaturation of Mb in the presence of crowding agents. This information is available free of charge via the Internet at http://pubs.acs.org

■ AUTHOR INFORMATION

Corresponding Author

*E-mail: pramitc@chemistry.iitd.ac.in.

Author Contributions

†These authors are equal contributors to the manuscript.

Notes

The authors declare no competing financial interest.

■ ACKNOWLEDGMENTS

A.M., J.K., and S.K.M. thank the Council of Scientific and Industrial Research (CSIR) and University Grants Commission (UGC), for their junior research fellowships. P.K.C. thanks the Department of Science and technology (DST), New Delhi, India, for financial support under the Fast Track Scheme for Young Scientists, IIT Delhi, for startup funding and Advanced Instrumentation Research Facility (AIRF), Jawaharlal Nehru University (JNU), for providing access to the time-resolved facility.

■ REFERENCES

(1) Ellis, R. J. *Trends Biochem. Sci.* **2001**, *26*, 597−604.
(2) Stagg, L.; Zhang, S.; Cheung, M. S.; Wittung-Stafshede, P. *Proc. Natl. Acad. Sci.* **2007**, *104*, 18976−18981.
(3) Zhou, H-X; Rivas, G.; Minton, A. P. *Annu. Rev. Biophys.* **2008**, *37*, 375−397.
(4) Minton, A. P. *Biophys. J.* **2005**, *88*, 971−985.
(5) Chebotareva, N. A.; Kurganow, B. I.; Livanova, N. B. *Biochemistry (Moscow)* **2004**, *69*, 1522−1536.
(6) Mukherjee, S.; Waegele, M. M.; Chowdhury, P.; Guo, L.; Gai, F. *J. Mol. Biol.* **2009**, *393*, 227−236.
(7) Munishkina, L. A.; Ahmad, A.; Fink, A. L.; Uversky, V. N. *Biochemistry* **2008**, *47*, 8993−9006.
(8) Philip, Y.; Sherman, E.; Haran, G.; Schreiber, G. *Biophys. J.* **2009**, *97*, 875−885.
(9) Berg, B. V. D.; Ellis, R. J.; Dobson, C. M. *EMBO J.* **1999**, *18*, 6927−6933.
(10) Banks, D. S.; Fradin, C. *Biophys. J.* **2005**, *89*, 2960−2971.
(11) Dauty, E.; Verkman, A. S. *J. Mol. Recog.* **2004**, *17*, 441−447.
(12) Lavalette, D.; Hink, M. A.; Tourbez, M.; Tetreau, C.; Visser, A. J. *Eur. Biophys. J.* **2006**, *35*, 517−522.
(13) Kozer, N.; Kotther, Y. Y.; Haran, G.; Schreiber, G. *Biophys. J.* **2007**, *92*, 213−2149.
(14) Cho, S. S.; Reddy, G.; Straub, J. E.; Thirumalai, D. *J. Phys. Chem. B* **2011**, *115*, 13401−13407.
(15) Wang, Y.; He, H.; Li, S. *Biochemistry* **2010**, *75*, 648−654.
(16) Despa, F.; Orgill, D. P.; Lee, R. C. *Ann. N. Y. Acad. Sci.* **2006**, *1066*, 54−66.
(17) Chiristiansen, A.; Wang, Q.; Samiotalus, A.; Cheung, M. S.; Wittung-Stafshede, P. *Biochemistry* **2010**, *49*, 6519−6530.
(18) Waegele, M. M.; Gai, F. *J. Chem. Phys.* **2011**, *134*, 95104(1−6).
(19) Schlesinger, A. P.; Wang, Y.; Tadeo, X.; Millet, O.; Pielak, G. J. *J. Am. Chem. Soc.* **2011**, *133*, 8082−8085.
(20) Samiotakis, A.; Wittung−Stafshede, P.; Cheung, M. S. *Int. J. Mol. Sci.* **2009**, *10*, 572−588.
(21) Dhar, A.; Samiotakis, A.; Ebbinghans, S.; Niehaw, L.; Homonz, D.; Gruebele, M.; Cheung, M. S. *Proc. Natl. Acad. Sci.* **2010**, *107*, 17586−17591.
(22) Zhou, H.-X. *Arch. Biochem. Biophys.* **2008**, *469*, 76−82.
(23) Eggers, D. K.; Valentine, J. S. *Protein Sci.* **2001**, *16*, 250−261.
(24) Zhou, H−X.; Dill, K. A. *Biochemistry* **2001**, *40*, 11289−11293.
(25) Zhou, H−X. *Acc. Chem. Res.* **2004**, *37*, 123−130.
(26) Takagi, F.; Koga, N.; Takada, S. *Proc. Natl. Acad. Sci.* **2003**, *20*, 11367−11372.
(27) Mittal, J.; Best, R. B. *Proc. Natl. Acad. Sci.* **2008**, *105*, 20233−20238.
(28) Sorin, E.; Pande, V. S. *J. Am. Chem. Soc.* **2006**, *128*, 6316−6317.
(29) Kendrew, J. C.; Bodo, G.; Dintzis, H. M.; Parrish, R. G.; Wyckoff, H. W.; Phillips, D. C. *Nature* **1958**, *181*, 662−666.
(30) Stevens, J. A.; Link, J. J.; Kao, Y−T; Zang, C.; Wang, L.; Zhong, D. *J. Phys. Chem. B* **2010**, *114*, 1498−1505.
(31) Venturoli, D.; Rippe, B. *Am. J. Physiol. Renal. Physiol.* **2005**, *288*, F605−F613.
(32) Vasquez, V. R.; Williams, B. C.; Graeve, O. A. *J. Phys. Chem. B* **2011**, *115*, 2979−2987.
(33) *Reverse micelles*; Luisi, P. L., Straub, B. E., Eds.; Plenum Press: New York, 1984.
(34) *Structure and reactivity in reverse micelles*; Pileni, M. P., Ed.; Elseiver: Amsterdam, 1989.
(35) Jain, T. K.; Varshney, M.; Maitra, A. *J. Phys. Chem.* **1989**, *93*, 7409−7416.
(36) Amararene, A.; Gindre, M.; Le Huerou, J-Y; Urabch, W.; Valdez, D.; Waks, M. *Phys. Rev. E* **2000**, *61*, 682−689.
(37) Kotlarchyk, M.; Huang, J. S.; Chen, S. H. *J. Phys. Chem.* **1985**, *89*, 4382−4386.
(38) Fändrich, M.; Forge, V.; Buder, K.; Kittler, M.; Dobson, C. M.; Diekmann, S. *Proc. Natl. Acad. Sci.* **2003**, *100*, 15463−15468.
(39) Tofani, L.; Feis, A.; Snoke, R. E.; Berti, D.; Baglioni, P.; Smulevich, G. *Biophys. J.* **2004**, *87*, 1186−1195.
(40) Kelly, S. M.; Jess, T. J.; Price, N. C. *Biochim. Biophys. Acta* **2005**, *1751*, 119−139.
(41) Murakami, H.; Nishi, T.; Toyota, Y. *J. Phys. Chem. B* **2011**, *115*, 5877−5885.
(42) Abel, S.; Waks, M.; Marchi, M. *Eur. Phys. J. E* **2010**, *32*, 399−409.
(43) Lucent, D.; Vishal, V.; Pande, V. S. *Proc. Natl. Acad. Sci.* **2007**, *104*, 10430−10434.
(44) Rosenfeld, D. E.; Schmuttenmaer, C. A. *J. Phys. Chem. B* **2006**, *110*, 14304−14312.
(45) Rosenfeld, D. E.; Schmuttenmaer, C. A. *J. Phys. Chem. B* **2011**, *115*, 1021−1031.
(46) Martinez, A. V.; Desensi, S. C.; Dominguez, L.; Rivera, E.; Straub, J. E. *J. Chem. Phys.* **2011**, *134*, 055107(1−9).
(47) Tian, J.; Garcia, A. E. *J. Chem. Phys.* **2011**, *134*, 225101−225111.
(48) Tian, J.; Garcia, A. E. *Biophys. J.* **2009**, *96*, L57−L59.
(49) Sakaue, T. *Macromolecules* **2007**, *40*, 5206−5211.
(50) Sengupta, A.; Khade, R. V.; Hazra, P. *J. Phys. Chem. A* **2011**, *115*, 10398−10407.
(51) Petrich, J. W.; Chang, M. C.; McDonald, D. B.; Fleming, G. R. *J. Am. Chem. Soc.* **1983**, *105*, 3824−3832.
(52) Anand, U.; Jash., C.; Mukherjee, S. *J. Phys. Chem. B* **2010**, *114*, 15839−15845.
(53) Anand, U.; Jash., C.; Mukherjee, S. *Phys. Chem. Chem. Phys.* **2011**, *13*, 20418−20426.
(54) Li, W.; Loong, C.; Thiyagarajan, P.; Lager, G.; Miranda, R. *J. Appl. Crystallogr.* **2000**, *33*, 628−631.
(55) Robertson, A. D.; Murphy, K. P. *Chem. Rev.* **1997**, *97*, 1251−1268.

(56) Homchaudhuri, L.; Sarma, N.; Swaminathan, R. *Biopolymers* **2006**, *83*, 477−486.
(57) Mukherjee, S.; Chowdhury, P.; Gai, F. *J. Phys. Chem. B* **2006**, *24*, 11615−11619.
(58) Babu, C. R.; Hilser, V. J.; Wand, A. J. *Nat. Struct. Mol. Biol.* **2004**, *11*, 352−357.
(59) Pometun, M. S.; Peterson, R. W.; Babu, C. R.; Wand, A. *J. Am. Chem. Soc.* **2006**, *128*, 10652−10653.
(60) Choi, J.; Terazima, M. *J. Phys. Chem. B* **2002**, *106*, 6587−6593.
(61) Dong, H.; Qin, S.; Zhou, H. X. *PLOS One Comput. Biol.* **2010**, *6*, e1000833(1−10).
(62) Harada, R.; Sugita, Y.; Feig, M. *J. Am. Chem. Soc.* **2012**, *134*, 4842−4849.